Accurate detection of dicrotic notch from PPG signal for telemonitoring applications

Abhishek Chakraborty,
Deboleena Sadhukhan and
Madhuchhanda Mitra*

Department of Applied Physics,
University College of Science and Technology (UCST),
University of Calcutta,
92 A.P.C. Road, Kolkata, 700-009, India
Email: ac.caluniv@yahoo.in
Email: dsaphy_rs@caluniv.ac.in
Email: mmaphy@caluniv.ac.in
*Corresponding author

Abstract: Recent technological advancement has inspired the modern population to adopt a portable, simple personal telemonitoring system that uses easy-to-acquire biosignal such as photoplethysmogram (PPG) for regular monitoring of vital signs. Consequently computerised analysis of PPG signal through accurate detection of clinically significant PPG fiducial points like dicrotic notch has become a key research area for early detection of physiological anomalies. In this research, a simple and robust algorithm is proposed for accurate detection of dicrotic notch from the PPG signal employing first and second derivative of the denoised signal, slope-reversal and an empirical formula-based approach. Features related to the dicrotic notch are then extracted from the baseline-corrected PPG signal and performance of the algorithm is evaluated over different standard PPG databases as well as over originally acquired signal. The algorithm achieves high efficiency in terms of sensitivity, positive predictivity, detection accuracy and low value of errors in the detected features.

Keywords: photoplethysmogram; PPG; amplitude threshold; slope reversal; dicrotic notch detection.

Reference to this paper should be made as follows: Chakraborty, A., Sadhukhan, D. and Mitra, M. (xxxx) 'Accurate detection of dicrotic notch from PPG signal for telemonitoring applications', *Int. J. Biomedical Engineering and Technology*, Vol. X, No. Y, pp.xxx–xxx.

Biographical notes: Abhishek Chakraborty received his BSc (Hons.) in Electronics and MSc in Electronic Science from the University of Calcutta, Kolkata, India in 2005 and 2007, respectively. He is currently pursuing his PhD at the Department of Applied Physics, University of Calcutta, India. He is also working as a part time Lecturer (government approved) from the Department of Electronics, Dum Dum Motijheel College, Kolkata since 2009. He has also qualified the UGC-NET (LS) examination in 2013. His research interests include biomedical signal processing and analysis.

Deboleena Sadhukhan received her BSc with major in Physics in 2007. She then completed her BTech and MTech in Instrumentation Engineering from the Department of Applied Physics, University of Calcutta, India in 2010 and 2012, respectively, and stood 1st class (gold medallist) in both of them. She is currently pursuing her PhD from the same department with the prestigious DST INSPIRE fellowship provided by the Department of Science and Technology, Government of India. Her research interests include biomedical signal processing and pattern recognition.

Madhuchhanda Mitra received her BTech, MTech and PhD (Tech.) in 1987, 1989 and 1998, respectively, from the University of Calcutta, Kolkata, India. At present, she is a Professor at the Department of Applied Physics, University College of Science and Technology, University of Calcutta, India, where she has been actively engaged in both teaching and research. She is the co-author of 150 research papers pertaining to the problems of biomedical signal processing, data acquisition and processing, fault analysis and material science. She is also a recipient of Griffith Memorial Award of the University of Calcutta.

1 Introduction

Over the past few years, aging issues, fast changing lifestyle and average increase in the stress related problems have resulted in the development of different chronic cardiovascular diseases among the population (Dai et al., 2016). On the contrary, regular access to the hospital-centred healthcare facilities is getting complicated day by day due to expenses, overpopulation and shortage of trained medical personnel (Baker et al., 2017). Furthermore, until date primary healthcare facilities in the rural areas are found to be in a terminally bad condition (Chandra et al., 2015). Consequently, the demand of low cost, easy-to-use telemonitoring facilities have become increasingly popular amongst fast-growing population, especially among the rural communities (Celler and Sparks, 2015). Recent advancements in the field of microelectronics and communication technologies have facilitated the development of such portable telemonitoring system for continuous and long-term monitoring of vital signs (Kim et al., 2016; Giorgio, 2015). However, the primary requirement of such telemonitoring system is to use a robust and easy biosignal acquisition technology, which allows full patient comfort.

Compared to other biosignal, photoplethysmogram (PPG) has been accepted widely in developing modern telemonitoring system because of its simple, portable and cost-effective acquisition technique (Yang et al., 1998). Contemporary PPG sensors uses a matched pair of light emitting diodes (LED) and photodetectors working at the near-infrared (NIR) wavelengths (0.8–1 μm). Hemoglobin absorbs the emitted light from the LED and the photo-detector measures backscattered light with respect to change in blood volume either in reflective mode or in transmission modes (Allen, 2007; Hertzman, 1937; Sundararajan, 2011). By nature, PPG is a low frequency (around 1 Hz) wave (Allen, 2007), which consists of a pulsatile ac component (signifies average blood volume change) superimposed on a quasi-DC component (representing respiration and sympathetic nervous activity, etc.). The onset of each pulse indicates the commencement of blood ejection from the heart to the aorta. The end of the ejection is manifested in the form of dicrotic notch, which also indicates closure of the aortic valve (Allen, 2007). Modern researches have focused on the use of different PPG-signal-features for the

estimation of several vital physiological parameters such as heart rate (Islam et al., 2017), blood oxygen saturation (Reddy et al., 2009), vascular assessment (Allen et al., 2006), cardiac output (Butter et al., 2004), hemodynamic stress (Sriraam et al., 2013), arterial stiffness (Reguig and Reguig, 2017), respiration (Chon et al., 2009) and blood pressure (He et al., 2014) to assess patient's health condition. Accurate estimation of different PPG features (such as pulse width, pulse area, peak to peak interval) requires an appropriate detection of different fiducial points such as pulse onset, systolic and diastolic peak and dicrotic notch. Hence, this is an important area of research in the field of automated health analysis systems using the PPG signal (Elgendi, 2012).

Among other PPG fiducial points the detection of dicrotic notch plays a prime role for analysis as it contains information to arterial stiffness (Shi et al., 2009), blood pressure (Gu et al., 2008), systemic vascular resistance (Lee et al., 2011) and atherosclerosis (Qawqzeh et al., 2010). However, the variant morphologies of dicrotic notch due to different pathological changes, such as aging, diabetic condition, atherosclerosis makes its detection quite challenging for computerised PPG analysis systems.

1.1 Literature review

Until date only a few dedicated algorithms/techniques have been proposed in the literature for the detection of dicrotic notch, addressing different levels of complexities. These methods can be broadly classified into two types:

1 morphological analysis of the PPG derivative

2 morphological analysis of the PPG signal itself.

However, signal analysis by means of derivative-based methods is usually noise sensitive. This makes pre-filtering of the signal as an essential step for further analysis. Morphological analysis of the PPG signal is also challenging due to the low frequency nature of the PPG signal and dependence of the PPG fiducial points on pathophysiological variations.

In Kyle et al. (1968), the authors first detected the steep upslope part of the pulse-onset and then a small upslope in the downward part of every pulse to identify the notch position. The algorithm was validated over 350 male subjects with age ranging from 15 to 88 years. But, the performance of the algorithm strongly depends on the quality of the pulse and the amount of high frequency artefacts present in the pulse. In Kinias et al. (1981), the authors located the dicrotic notch by creating two chords of decreasing length around a bend-point in the pulse waveform. The algorithm was tested over 1,005 cycles with two false positive cycles. Oppenheim and Sittig (1995) later modified the algorithm proposed in Kinias et al. (1981) by combining it with a derivative-based approach. However, this algorithm was evaluated only over a very small-scale dataset of 373 beats from eight patients. In Blazek and Lee (2010), the authors proposed a weighted broken-stick model with different scales and forms in sequence to identify the dicrotic notch points. Li et al. (2010) detected the dicrotic notch location by identifying the inflection and zero-crossing points in the first-derivative of the signal. The obtained sensitivity and positive predictivity for the detection of dicrotic notch are found to be 96.53% and 96.64% respectively. In Hoeksel et al. (1997) and Donelli et al. (2002), the authors identified dicrotic notch using a simplified windkessel model and evaluated the performance of their algorithm on the dataset obtained from

animals and chosen patients. In addition, their models (Hoeksel et al., 1997; Donelli et al., 2002) depend on several heuristically-chosen physiological parameters such as characteristic impedance, arterial compliance and peripheral resistance which might not be appropriate for all the subjects. The algorithm proposed in Shi et al. (2009) analyses PPG contour between the maximum and the following minimum, i.e., local minimum in the waveform to detect prominent dicrotic notch locations. Although the algorithm was tested on PPG data records acquired from young adults only.

Acceleration PPG (SDPPG) signal allows easier interpretation of the PPG waveform by enhancing several clinically important feature-zones. It consists of four systolic waves (*a*, *b*, *c* and *d* waves) and one diastolic wave (*e* wave) (Elgendi, 2012) related to the dicrotic notch. In Soundararajan et al. (2016), dicrotic notch is identified by exploiting the SDPPG *e* wave; but the algorithm requires a secondary signal like the ECG to validate the beat detection accuracy. Additionally, the used database was very small, containing 707 beats from 46 records. In Elgendi (2014), a method is proposed by generating blocks of interest based on two moving average filters followed by dynamic event duration threshold to identify *c*, *d* and *e* waves in the SDPPG signal. The algorithm was validated over 27 records obtained from young and healthy adults only.

Most of these algorithms were validated over a very small dataset (Kinias et al., 1981; Donelli et al., 2002; Hoeksel et al., 1997; Oppenheim and Sittig, 1995; Shi et al., 2009; Soundararajan et al., 2016; Elgendi, 2014) and only a few of them dealt with the pathological variations in the signal (Donelli et al., 2002; Hoeksel et al., 1997; Oppenheim and Sittig, 1995).

To the best knowledge of the authors of this article, no dedicated literature has been proposed till date focusing on the extraction of dicrotic notch location from both healthy and pathological data having significant morphological and pathological variations. So the main goal of this paper is to propose a robust, accurate yet simple algorithm for precise identification of PPG dicrotic notch followed by relevant notch related features extraction. Here first derivative (FDPPG) and second derivative (SDPPG) of the PPG signal is calculated at first. Then an empirically determined formula is used to identify the dicrotic notch location accurately. The proposed algorithm is also validated extensively over a large number of normal and pathological data as obtained from different databases and also on the data collected from both healthy volunteers and cardiac patients. The rest of this paper is organised as follows. The proposed dicrotic notch detection algorithm is presented in Section 2. The experimental result is presented in Section 3 and a detail discussion about the robustness and efficiency of the algorithm is presented in Section 4. Finally, the conclusions are drawn along with possible future work prediction in Section 5.

2 Methodology

The proposed methodology consists of the major parts as shown in Figure 1.

Figure 1 Schematic diagram of the proposed algorithm

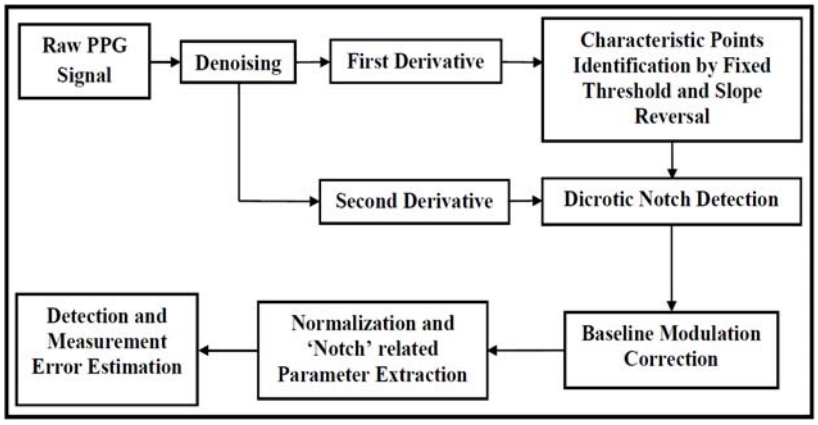

Notes: The algorithm consists of two stages: dicrotic notch detection (based on amplitude thresholding, slope-reversal and an empirical formula-based approach), and then notch related feature extraction.

2.1 PPG preprocessing

PPG signal amplitude is influenced by the light at the photo-detector, poor blood perfusion of the peripheral tissues and different types of motion artefacts, which may cause signal deterioration (Sukor et al., 2011). Since the algorithm follows derivative-based methods, consequently it becomes noise sensitive. Hence, for the proposed method the digitally acquired PPG signals are filtered using a sixth order Butterworth low-pass filter with a cut-off frequency of 15 Hz, to remove the high frequency noises.

2.2 PPG derivatives computation

The first (FDPPG) and second derivative (SDPPG) of the denoised PPG signal is then computed using the following equations

$$FDPPG = \frac{d}{dt}(V_{PPG}) = \frac{d}{dt}\left[y(t+1) - y(t)\right] \tag{1}$$

$$SDPPG = \frac{d}{dt}(FDPPG) = \frac{d}{dt}\left[y(t+1) + y(t-1) - 2y(t)\right] \tag{2}$$

where $y(t)$ is the present sample and $y(t-1)$ and $y(t+1)$ represent the previous and the next sample, respectively. Usually, the first derivative of the signal is considered as equivalent to the high pass filter. That means it essentially removes the low frequency components and enhances the high slope regions in the signal. This in turn improves the detection accuracy of various characteristics points.

2.3 Identification of characteristic points

At first, the FDPPG waveform is analysed to identify FDPPG maximum and minimum peaks. To calculate dicrotic notch related features accurately, PPG onset and systolic peaks are located with the help of FDPPG maximum peak. Then FDPPG local extreme point is identified and dicrotic notch location is extracted accurately using FDPPG local extreme point, FDPPG minimum peak and SDPPG signal. The methodology is described in detail as follows.

2.3.1 Detection of FDPPG maximum peak

Primarily based on the amplitude range, the whole FDPPG signal is subjected to a fixed threshold value. The threshold percentage is empirically chosen after extensive tests on different types of FDPPG data. In this case, amplitude threshold of 50% of the FDPPG signal amplitude range is chosen to identify the higher amplitude regions. FDPPG maximum peaks are then accurately identified from these selected regions by searching for the slope reversal points within fixed windows as shown in Figure 2(a).

2.3.2 Detection of FDPPG minimum peak

It is noted that FDPPG minimum peaks are usually located in the starting of the region between two consecutive FDPPG maximum peak locations. So that, the amplitude range in the first half portion is subjected to another empirically chosen threshold value of 80% as shown in Figure 2(b). This approach not only narrows down the relevant search area but also eliminates the possibility of selecting any other local minima point between two consecutive FDPPG maximum peak locations other than the actual FDPPG minimum peak. FDPPG minimum peaks are then identified from these selected regions by searching for slope reversal points within fixed windows.

Figure 2 (a) Samples with amplitudes greater than a pre-determined threshold value are marked to identify maximum peaks and (b) Samples in the starting of the region between two FDPPG maximum peaks with amplitudes less than a pre-determined threshold value are marked to identify minimum peaks in the FDPPG plot (c) Detected FDPPG maximum peaks are indicated by square symbol and the FDPPG minimum peaks are indicated by circle

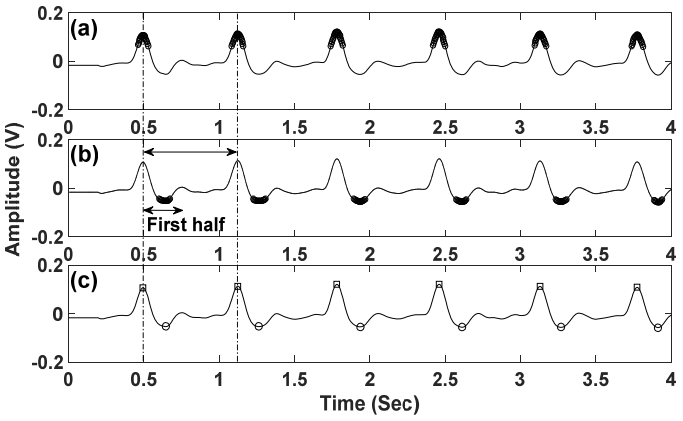

Generally, human heart rate under maximum variation cannot exceed a highest value of 240 per minute (Mukhopadhyay et al., 2012). This corresponds to four beats per second which leads to a minimum beat interval of 0.25 second. Hence, in order to determine FDPPG maximum and minimum peaks accurately without having a chance of identifying any false peak the window size is kept fixed to 0.25 second. The whole operation of maximum and minimum peak detection is summarised in Figure 2.

2.3.3 PPG first derivative local extreme point detection

At first, a region of interest is created starting from the FDPPG minimum-peak index up to the next FDPPG zero crossing point. Then 70% samples are chosen within this interval starting from the FDPPG minimum-peak location. The percentage of samples to be taken within this interval is determined based on a trial and error method as shown in Figure 3. Finally, the index of FDPPG local extreme is identified within these boundary points using an empirical formula as described below. In Figure 3, the minimum peak value is marked as (a_1, b_1) and the chosen 70% distant sample point as (a_2, b_2), where (a_1, a_2) represent the time values and (b_1, b_2) represent the corresponding voltage values. Now the amplitude of all the FDPPG samples between these two points are altered by the empirical formula as stated in equation (3).

$$Modified\ FDPPG\ sample = \left[(Original\ sample) - m \times i - b_1\right] \tag{3}$$

Here, m is the slope between (a_1, b_1) and (a_2, b_2) points and $m = \left(\frac{b_2 - b_1}{a_2 - a_1}\right)$.

Figure 3 Local extreme point detection between the FDPPG minimum-peak and the next zero crossing point using an empirical formula

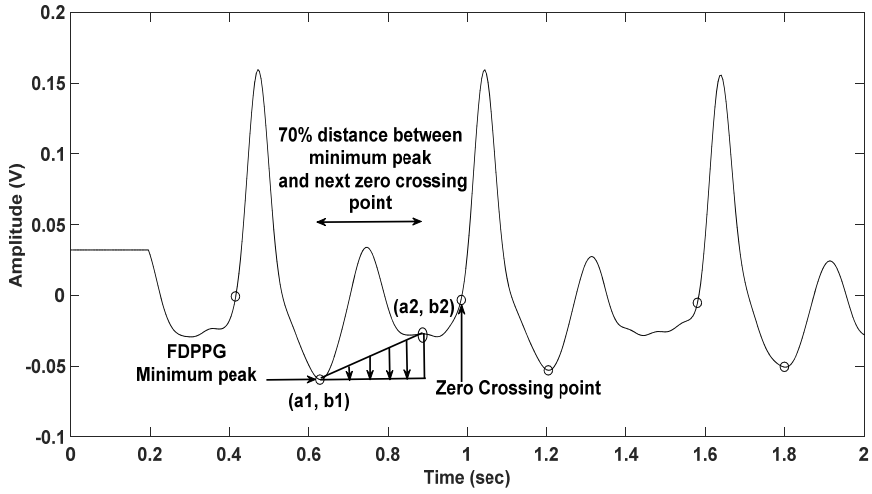

In equation (3), the value of i is initially set to zero and then it is incremented step by step as per the sampling interval of the signal. The slope factor m is used to bring down each FDPPG sample to the same level as the starting point (a_1, b_1). Finally, b_1 is subtracted to

create modified FDPPG signal with a starting point of zero voltage. Now, maximum peak location of the modified FDPPG signal is determined at first. Then taking reference to the location of this maximum peak, a slope-reversal or slope-change point is identified in the original FDPPG signal as the location of local extreme point as shown in Figure 4.

Figure 4 Encircled local extreme points for two different types of FDPPG signal

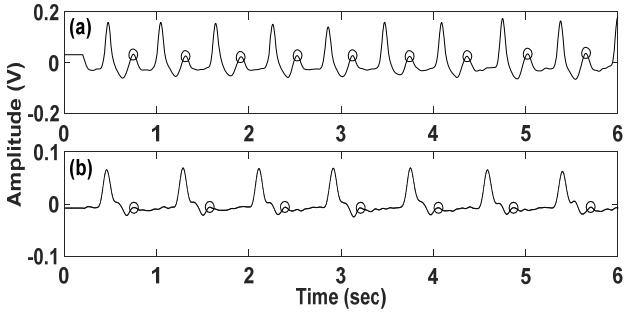

2.3.4 Pulse onset and systolic peak detection

It has already been well established that any singularity in a differentiable signals must correspond to a pair of inflection and zero-crossing points in the derivative of that signal (Mallat and Hwang, 1992). Usually the zero-crossing point in a FDPPG signal before a maximal inflection is related to the pulse onset, whereas zero crossing point after inflection is related to the systolic peak of the PPG signal. Considering the most recently detected FDPPG maximum peak as reference, left and right traversal in the FDPPG data is carried out to identify first and second zero crossing points as shown in Figure 5(a). Now, 20 samples of the original PPG signal around each of such zero crossing point indices are marked to create an effective search zone as shown in Figure 5(b). Slope reversal point among these marked samples around the first zero crossing points are then identified to be the precise location of pulse onset point. Similarly slope reversal point among those marked samples around the second zero crossing points is identified as the precise location of systolic peak as depicted in Figure 5(c).

2.3.5 Dicrotic notch identification

The detected FDPPG minimum peak and the local extreme point indices are mapped on the SDPPG signal. Now starting from the FDPPG local extreme point location index a left search is carried out on the SDPPG signal up to the FDPPG minimum point location index till a slope reversal point is found and identified as the *e* wave. The identified *e* wave index is plotted to the original PPG signal to get the accurate location of the dicrotic notch as depicted in Figure 6(a). An intense trial over a large variety of normal and diseased data suggests that despite of several pathophysiological varieties, these two FDPPG characteristic points facilitates effortless, precise and easy identification of *e* wave location without SDPPG signal analysis which leads to accurate identification of dicrotic notch as illustrated in Figure 6.

Figure 5 (a) First zero-crossing points before the inflections are indicated by circle-symbols and second zero-crossing points after-inflections are marked using square-symbols (b) Twenty samples are mapped on the original PPG signal taking reference to each of those zero crossing point indices (c) Identified pulse onset points are indicated by circle and identified systolic peaks are marked using square symbols

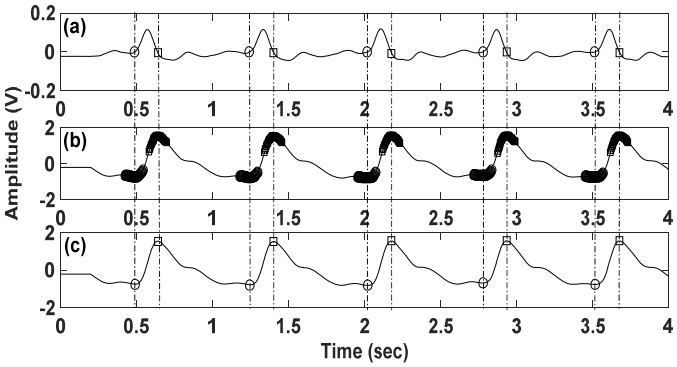

Figure 6 (a) Detected dicrotic notch points are encircled in the original PPG signal (b) Encircled minimum peak and local extreme points in the FDPPG signal (c) Encircled middle point indicate the location of 'e' wave, between the location of minimum peak (left star) and local extreme point (right star) in the SDPPG signal

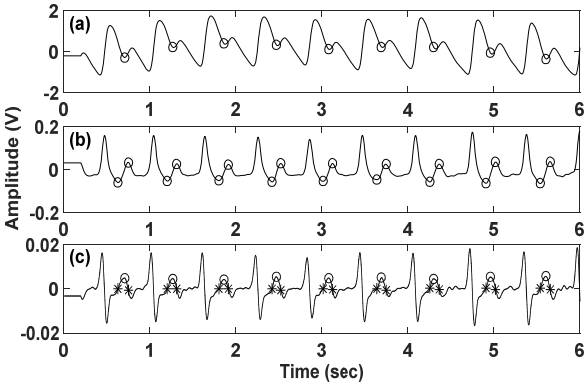

2.4 Baseline modulation correction

Sometimes due to irregular breathing, noises caused by body movement during data acquisition and as a result of poor finger tip contact on the sensor, baseline wander occurs in the PPG signal even within a single beat duration as can be seen from different PPG cycles of Figure 7(a). Since all the amplitude features are calculated with respect to a common base value, any uneven signal fluctuation might feed us wrong feature values. To resolve this, the identified first pulse onset point is chosen as the baseline point of each cardiac beat as indicated in an example beat of Figure 7(a). Then each sample in between the consecutive onset points is modified using the same empirical formula as

stated in equation (3). Here also the variable i is incremented from zero as per the sampling interval of the PPG signal. Finally, b_1 is subtracted to have zero voltage at the baseline points.

After baseline correction, to be able to evaluate the same feature variation among different subject, the baseline corrected PPG signal data is amplitude normalised in the range 0–1 using equation (4).

$$V_{Norm} = \frac{\left(V_{PPG} - V_{PPG(\mathrm{Min})}\right)}{\left(V_{PPG(\mathrm{Max})} - V_{PPG(\mathrm{Min})}\right)} \tag{4}$$

Here, V_{PPG} = baseline corrected PPG signal, $V_{PPG(\mathrm{Min})}$ = minimum value of the baseline corrected PPG signal, $V_{PPG(\mathrm{Max})}$ = maximum value of the baseline corrected PPG signal.

Now after baseline modulation correction and normalisation, the height and duration parameters of all the dicrotic notch points are measured using the following formula.

Dicrotic notch amplitude = voltage difference between notch point and X-axis in normalised unit (NU) and dicrotic notch duration = time difference between notch and pulse onset point in seconds.

Typical amplitude normalised PPG signal before and after baseline modulation correction is shown in Figures 7(a) and 7(b) respectively.

Figure 7 (a) Amplitude normalised PPG signal record before baseline modulation correction (b) Same PPG signal after baseline modulation correction

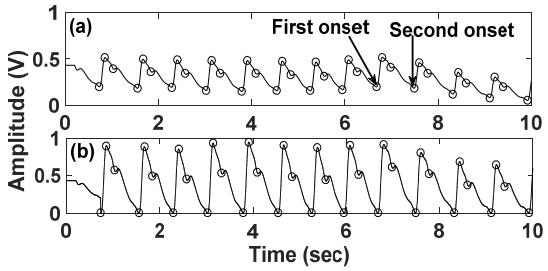

2.5 Detection and measurement error estimation

Visual inspection of all the records suggests that the dicrotic notch amplitude and location in a particular PPG record often deviates from cycle to cycle, which appears in the form of notch amplitude and duration measurement error. In this research, absolute amplitude measurement error is measured as the percentage of average differences of each calculated notch height with the earlier, the absolute duration measurement error is measured as the percentage of average differences of each calculated notch duration with the earlier and is represented in Table 1.

3 Experimental results

The developed algorithm was validated extensively over a large number of PPG records from five different databases:

a the CapnoBase database which contains 42 records of different signals including PPG (sampling frequency 300 Hz) collected from 29 pediatric and 13 adults (Karlen et al., 2013)

b the University of Queensland vital signs dataset, with multiple vital signal recordings including PPG of 32 cases (sampling frequency 100 Hz) (Liu et al., 2012)

c the MIMIC database, which includes PPG data records (sampling frequency 500 Hz) collected from over 90 ICU patients (Goldberger et al., 2000)

d real time PPG signal data (sampling frequency 250 Hz) acquired using BIOPAC MP 45 at 250 Hz sampling frequency from 60 healthy subjects

e also from 50 patients, admitted in the cardiology ward of Medical College and Hospital, Kolkata along with written informed consent from each subject.

Overall performance of this proposed algorithm is assessed by means of three benchmark statistical parameters defined as follows:

$$Sensitivity\ (SE) = \frac{TP}{TP + FN} \times 100\% \tag{5}$$

$$Positive\ predictivity\ (PP) = \frac{TP}{TP + FP} \times 100\% \tag{6}$$

$$Detection\ acuracy\ (Acc) = \frac{TP}{TP + FN + FP} \times 100\% \tag{7}$$

where

TP number of true positives (notch location identified as notch)

FN number of false negatives (notch location which have not been identified)

FP number of false positives (non-notch point is identified as notch)

SE percentage of true beats that are correctly detected by the algorithm

PP percentage of beats detected by the algorithm that are true.

Since the used databases are not annotated, the point locations detected by the algorithm are cross validated using visual inspection by experienced medical practitioner. Few selected records from each database have been shown in Table 1. Also, the average values of the parameters as calculated from all the beats from each database are listed. The proposed algorithm offers significantly high efficiency in terms of average sensitivity (99.42%), positive predictivity (100%), and detection accuracy (99.42%). The average normalised notch amplitude detection error (6.336%) and duration detection error (4.370%) among five databases are found to be within permissible limit as presented in Table 1.

In addition, the proposed algorithm takes around five seconds to process almost 15,000 samples of a single record using 'MATLAB' on a desktop PC having a Pentium core i3 CPU with 4 GB RAM. This approximate time assessment suggests that the algorithm can be used for intermittent online applications as well.

Table 1 Overall performance of the proposed algorithm

CapnoBase data											
Record no.	*Total beats*	*TP*	*FN*	*FP*	*Se (%)*	*PP (%)*	*Acc (%)*	*Average of notch amplitude in normalized unit (NU)*	*Average amplitude detection error (%)*	*Average notch duration (second)*	*Average duration detection error (%)*
103	104	104	0	0	100	100	100	0.522	5.982	0.277	0.945
127	85	85	0	0	100	100	100	0.095	2.266	0.368	1.468
142	95	94	1	0	98.95	100	98.95	0.144	3.371	0.391	2.788
329	114	114	0	0	100	100	100	0.200	2.703	0.325	0.631
Average	3,460	3,376	84	0	97.57	100	97.57	0.320	7.808	0.409	5.033
University of Queensland vital signs dataset											
Case_01	55	55	0	0	100	100	100	0.104	3.614	0.453	4.269
Case_03	72	71	1	0	98.61	100	98.61	0.089	2.391	0.503	4.072
Case_07	62	62	0	0	100	100	100	0.342	5.110	0.407	3.983
Case_16	42	0	0	0	100	100	100	0.032	1.766	0.439	1.897
Average	2,010	2,008	2	0	99.90	100	99.90	0.272	6.611	0.440	4.623
MIMIC data											
3900001	122	120	2	0	98.36	100	98.36	0.059	3.696	0.287	0.998
5500003	101	101	0	0	100	100	100	0.280	1.560	0.287	0.341
21200002	81	81	0	0	100	100	100	0.473	3.550	0.326	1.108
23700080	75	75	0	0	100	100	100	0.119	2.724	0.308	1.351
Average	6,403	6,394	9	0	99.85	100	99.85	0.283	4.805	0.382	3.324
Laboratory acquired normal data											
32	72	70	2	0	97.22	100	97.22	0.527	4.541	0.313	2.382
47	83	83	0	0	100	100	100	0.524	4.414	0.321	2.415
58	69	69	0	0	100	100	100	0.605	4.401	0.328	1.473
64	74	74	0	0	100	100	100	0.629	4.345	0.323	1.442
Average	5,116	5,104	12	0	99.76	100	99.76	0.408	5.637	0.369	4.098
Hospital acquired cardiovascular patient data											
10	108	107	1	0	99.07	100	99.07	0.222	4.303	0.267	1.170
12	111	111	0	0	100	100	100	0.084	4.996	0.251	1.552
38	104	104	0	0	100	100	100	0.419	5.881	0.331	3.616
73	99	99	0	0	100	100	100	0.567	6.980	0.329	2.838
Average	3,263	3,253	10	0	99.69	100	99.69	0.38	6.82	0.35	4.77
Average performance of all data											
Average	20,252	20,135	117	0	99.42	100	99.42	0.333	6.336	0.390	4.370

4 Discussions

Detection of PPG dicrotic notch is very challenging, due to the low frequency nature of the PPG signal and dependence of the dicrotic notch point on pathological variations. However, compared to other existing methods, the proposed algorithm efficiently identifies the dicrotic notch locations on the PPG records collected from different standard databases and also on the PPG data collected from both healthy and cardiac patients, as seen in Table 1. In addition, pulse onset and systolic peaks are successfully detected by the algorithm and some important PPG dicrotic notch related features are extracted after baseline modulation correction as listed in Table 1. The algorithm employs derivative-based method instead of any computationally complex transform-based techniques. With little effort, the algorithm can be modified and enhanced to determine other important PPG characteristics-points and features (e.g., diastolic peak, half width points, pulse width, pulse area, etc.) towards the development of a complete PPG feature extraction system.

Since the applied derivative-based approach makes the algorithm noise sensitive, hence proper denoising is required at the preprocessing stage. It can be seen from Figure 7 that the algorithm fails to rectify the baseline-modulation of the first PPG cycle if the first sample of the PPG data belongs to any other part other than the onset point of a particular cycle. The same conclusion can also be drawn for the last cycle. Further, it is seen that, PPG records with extremely low amplitude or PPG records containing sudden high amplitude spikes significantly affect the performance of the algorithm as it will alter the threshold values.

Based on available literatures, a reasonable performance comparison of the proposed technique with relevant works is presented in Table 2. The comparison reveals that with respect to the number of beats used, our algorithm outperforms the others. Although differences in used datasets, validation, number of beats and differences in evaluation parameters in the previous studies present serious obstacle for exact comparison. Different PPG waves from different databases that are identified by the proposed algorithm are shown in Figure 8.

Table 2 Comparison of the proposed method with previous studies

Publications	*Method used*	*Beats*	*Se (%)*	*PP (%)*
Kinias et al. (1981)	Bend-point algorithm	1,005	99.90	99.80
Oppenheim and Sittig (1995)	Signal derivative	373	99.46	96.86
Li et al. (2010)	First derivative	2,564	96.53	96.64
Soundararajan et al. (2016)	Zero crossing detection in the SDPPG wave	707	99.67	99.82
Elgendi (2014)	Event-related moving averages	584	99.64	99.64
Proposed	First and second derivative	20,252	99.42	100

Our current research focus is to enhance and modify the present PPG dicrotic notch detection algorithm, so that it can extract all possible features from the PPG signal. The enhanced algorithm has already been implemented and verified on the software level. The final goal is to implement the algorithm in an embedded platform, so that, through

suitable interfacing with a PPG acquisition module, the device can act as a prototype PPG monitoring tool and can be used for analysis of different cardiac diseases using the extracted features.

Figure 8 PPG signal from (a) CapnoBase database, (b) University of Queensland vital signs dataset, (c) MIMIC database, (d) normal database, and (e) Cardiovascular patient database

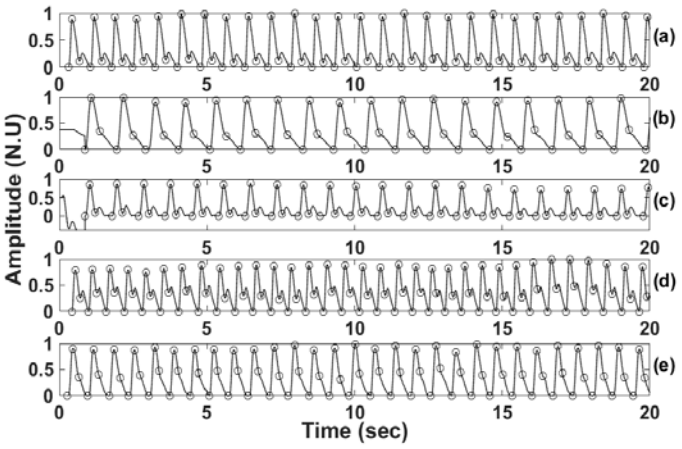

5 Conclusions

Recently, PPG signals are popularly used in several low cost, easy-to-use telemonitoring devices where different PPG signal features are efficiently used to identify human health condition. This makes PPG characteristic points and hence PPG feature extraction as the most crucial step. Although it is seen that, out of several important feature points, detection of dicrotic notch is the most vital and complicated as its nature varies rapidly with pathophysiological variations. To the best knowledge of the authors of this article, no such algorithm is proposed till date which can extract accurate dicrotic notch location from both healthy and pathological PPG data having significant morphological and pathological variations and which is computationally simple enough for implementation in an embedded platform.

In this paper, a robust, accurate yet simple technique is proposed to identify the locations of the dicrotic notch in the PPG signal. The proposed algorithm is presented in two steps: dicrotic notch detection using simple mathematical methods followed by relevant notch related features extraction. The technique is based on using the combination of the first and second derivative of the PPG signal and finally applying slope-reversal search and an empirical formula-based approach. The proposed technique does not rely on any transform-based operations. Instead, it relies on simple signal derivative calculation and threshold-based methods. This, in turn, makes the algorithm computationally simple and hence ensures easy implementation in embedded platforms of the portable telemonitoring devices. The algorithm is extensively evaluated with a huge variety of PPG records including both healthy and abnormal data. The extracted

characteristic points are cross validated through visual inspection by experienced medical practitioners. The significantly high detection accuracy obtained for all the records proves the robustness of the algorithm for the wide pathological variation, amplitude fluctuation and morphological diversity including sampling rate. The algorithm can be further extended to develop complete PPG analysis software for the telemonitoring devices which will employ the different extracted PPG features to identify the health abnormalities.

Acknowledgements

The authors would like to express their deepest gratitude to Dr. S. Guha (HOD), other medical practitioners and the entire support staffs of the department of cardiology, Medical College and Hospital, Kolkata for their valuable suggestions and assistance in the development of PPG database and validation of the proposed algorithm.

References

Allen, J. (2007) 'Photoplethysmography and its application in clinical physiological measurement', *Physiological Measurement*, Vol. 28, No. 3, pp.1–39.

Allen, J., Overbeck, K., Stansby, G. and Murrey, A. (2006) 'Photoplethysmography assessments in cardiovascular disease', *Measurement and Control*, Vol. 39, No. 3, pp.80–83.

Baker, S.B., Xiang, W., and Atkinson, I. (2017) 'Internet of things for smart healthcare: technologies, challenges, and opportunities', *IEEE Access*, Vol. 5, pp.26521–26544, DOI: 10.1109/ACCESS.2017.2775180.

Blazek, R. and Lee, C. (2010) 'Multi-resolution linear model comparison for detection of dicrotic notch and peak in blood volume pulse signals', in *20th International EURASIP Conference, Biosignal*; Czech Republic, pp.378–386.

Butter, C., Stellbrink, C., Belalcazar, A., Villalta, D., Schlegl, M., Sinha, A., Cuesta, F. and Reister, C. (2004) 'Cardiac resynchronization therapy optimization by finger plethysmography', *Heart Rhythm*, Vol. 1, No. 5, pp.568–575.

Celler, B.G. and Sparks, R.S. (2015) 'Home telemonitoring of vital signs – technical challenges and future directions', *IEEE Journal of Biomedical and Health Informatics*, Vol. 19, No.1, pp.82–91.

Chandra, B.S., Sastry, C.S. and Jana, S. (2015) 'Reliable resource-constrained telecardiology via compressive detection of anomalous ECG signals', *Computers in Biology and Medicine*, Vol. 66, pp.144–153, DOI: 10.1016/j.compbiomed.2015.09.005.

Chon, K.H., Dash, S. and Ju, K. (2009) 'Estimation of respiratory rate from photoplethysmogram data using time-frequency spectral estimation', *IEEE Transactions on Biomedical Engineering*, Vol. 56, No. 8, pp.2054-2063.

Dai, M., Xiao, X., Chen, X., Lin, H., Wu, W. and Chen, S. (2016) 'A low-power and miniaturized electrocardiograph data collection system with smart textile electrodes for monitoring of cardiac function', *Australasian Physical and Engineering Sciences in Medicine*, Vol. 39, pp.1029–1040, DOI: 10.1007/s13246-016-0483-5.

Donelli, A., Jansen, J.R., Hoeksel, B., Pedeferri, P., Hanania, R. and Bovelander, J. (2002) 'Performance of a real-time dicrotic notch detection and prediction algorithm in arrhythmic human aortic pressure signals', *Journal of Clinical Monitoring and Computing*, Vol. 17, Nos. 3–4, pp.181–185.

Elgendi, M. (2012) 'On the analysis of fingertip photoplethysmogram signals', *Current Cardiology Reviews*, Vol. 8, No. 1, pp.14–25.

Elgendi, M. (2014) 'Detection of c, d, and e waves in the acceleration photoplethysmogram', *Computer Methods and Programs in Biomedicine*, Vol. 117, pp.125–136, DOI: 10.1016/j.cmpb.2014.08.001.

Giorgio, A. (2015) 'A wireless electronic device for the personal safety of chronically ill persons for indoor and outdoor use', *International Journal of Biomedical Engineering and Technology*, Vol. 18, p.72, DOI: 10.1504/IJBET.2015.069853.

Goldberger, A.L., Amaral, L.A., Glass, L., Hausdorff, J.M., Ivanov, P.C., Mark, R.G., Mietus, J.E., Moody, G.B., Peng, C.K. and Stanley, H.E. (2000) 'PhysioBank, PhysioToolkit, and PhysioNet: components of a new research resource for complex physiologic signals', *Circulation*, Vol. 101, No. 23, pp.215–220.

Gu, W.B., Poon, C.C.Y. and Zhang, Y.T. (2008) 'A novel parameter from PPG dicrotic notch for estimation of systolic blood pressure using pulse transit time', *5th International Summer School and Symposium on Medical Devices and Biosensors*, Hong Kong, pp.86–88.

He, X. Goubran, R.A. and Liu, X.P. (2014) 'Secondary peak detection of PPG signal for continuous cuffless arterial blood pressure measurement', *IEEE Transactions on Instrumentation and Measurement*, Vol. 63, No. 6, pp.1431–1439.

Hertzman, A.B. (1937) 'Photoelectric plethysmography of the fingers and toes in man', *Experimental Biology and Medicine*, Vol. 37, No. 3, pp.529–534.

Hoeksel, S.A., Jansen, J.R., Blom, J.A. and Schreuder, J.J. (1997) 'Detection of dicrotic notch in arterial pressure signals', *Journal of Clinical Monitoring*, Vol. 13, No. 5, pp.309–316.

Islam, M.T., Zabir, I., Ahamed, S.T., Yasar, M.T., Shahnaz, C. and Fattah, S.A. (2017) 'A time-frequency domain approach of heart rate estimation from photoplethysmographic (PPG) signal', *Biomedical Signal Processing and Control*, Vol. 36, pp.146–154.

Karlen, W., Raman, S., Ansermino, J.M. and Dumont, G.A. (2013) 'Multiparameter respiratory rate estimation from the photoplethysmogram', *IEEE Transactions on Biomedical Engineering*, Vol. 60, No. 7, pp.1946–1953.

Kim, Y., Lee, S. and Lee, S. (2016) 'Coexistence of ZigBee-based WBAN and WiFi for health telemonitoring systems', *IEEE Journal of Biomedical and Health Informatics*, Vol. 20, No.1, pp.222–230.

Kinias, P., Fozzard, H.A. and Norusis, M.J. (1981) 'A real-time pressure algorithm', *Computers in Biology and Medicine*, Vol. 11, No. 4, pp.211–220.

Kyle, M.C., Klingeman, J.D. and Freis, E.D. (1968), 'Computer identification of brachial arterial pulse waves', *Computers and Biomedical Research*, Vol. 2, No. 2, pp.151–159.

Lee, Q.Y., Chan, G.S., Redmond, S.J., Middleton, P.M., Steel, E., Malouf, P., Critoph, C., Flynn, G., O'Lone, E. and Lovell, N.H. (2011) 'Multivariate classification of systemic vascular resistance using photoplethysmography', *Physiological Measurement*, Vol. 32, No. 8, pp.1117–1132.

Li, B.N., Dong, M.C. and Vai, M.I. (2010) 'On an automatic delineator for arterial blood pressure waveforms', *Biomedical Signal Processing and Control*, Vol. 5, No.1, pp.76–81.

Liu, D., Görges, M., and Jenkins, S.A. (2012) 'University of Queensland vital signs dataset: development of an accessible repository of anesthesia patient monitoring data for research', *Anesthesia and Analgesia*, Vol. 114, No. 3, pp.584–589 [online] https://doi.org/10.1213/ANE.0b013e318241f7c0.

Mallat, S. and Hwang, W.L. (1992) 'Singularity detection and processing with wavelets', *IEEE Transactions on Information Theory*, Vol. 38, No. 2, pp.617–643.

Mukhopadhyay, S.K., Mitra, M. and Mitra, S. (2012) 'ECG feature extraction using differentiation, Hilbert transform, variable threshold and slope reversal approach', *Journal of Medical Engineering and Technology*, Vol. 36, pp.372–386, DOI: 10.3109/03091902.2012.713438.

Oppenheim, M.J. and Sittig, D.F. (1995) 'An innovative dicrotic notch detection algorithm which combines rule-based logic with digital signal processing techniques', *Computers and Biomedical Research*, Vol. 28, No. 2, pp.154–170.

Qawqzeh, Y.K., Reaz, M.B.I. and Ali, M.A.M. (2010) 'The analysis of PPG contour in the assessment of atherosclerosis for erectile dysfunction subjects', *WSEAS Transactions on Biology and Biomedicine*, Vol. 7, No. 4, pp.306–315.

Reddy, K.A., George, B., Mohan, N.M. and Kumar, V.J. (2009) 'A novel calibration-free method of measurement of oxygen saturation in arterial blood', *IEEE Transactions on Instrumentation and Measurement*, Vol. 58, pp.1699–1705, DOI: 10.1109/tim.2009.2012934.

Reguig, M.A.B. and Reguig, F.B. (2017) 'Photoplethysmogram signal processing and analysis in evaluating arterial stiffness', *International Journal of Biomedical Engineering and Technology*, Vol. 23, p.363, DOI: 10.1504/IJBET.2017.082674.

Shi, P., Hu, S., Zhu, Y., Zheng, J., Qiu, Y. and Cheang, P.Y. (2009) 'Insight into the dicrotic notch in photoplethysmographic pulses from finger tip of young adults', *Journal of Medical Engineering & Technology*, Vol. 33, No. 8, pp.628–633.

Soundararajan, M., Arunagiri, S. and Alagala, S. (2016) 'An adaptive delineator for photoplethysmography waveform', *Biomedical Engineering/Biomedizinische Technik*, Vol. 61, No. 6, pp.645–655.

Sriraam, N., Pradhapan, P., Swaminathan, M. and Mohan, H.K.S.V. (2013) 'Comparison of MLP and REN classifiers for detection of hemodynamic stress using photoplethysmograph', *International Journal of Biomedical Engineering and Technology*, Vol. 12, p.97, DOI: 10.1504/IJBET.2013.056287.

Sukor, J.A., Redmond, S.J. and Lovell, N.H. (2011) 'Signal quality measures for pulse oximetry through waveform morphology analysis', *Physiological Measurement*, Vol. 32, No. 3, pp.369–384.

Sundararajan, M. (2011) 'Optical instrument for correlative analysis of human ECG and breathing signal', *International Journal of Biomedical Engineering and Technology*, Vol. 6, p.350, DOI: 10.1504/IJBET.2011.041773.

Yang, B.H., Rhee, S. and Asada, H.H. (1998) 'A twenty-four hour tele-nursing system using a ring sensor', *IEEE International Conference on Robotics and Automation*, Vol. 1 pp.387–392.